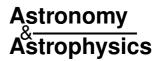
DOI: 10.1051/0004-6361:20020832

© ESO 2002



Large-scale asymmetry of rotation curves in lopsided spiral galaxies

C. J. Jog*

Department of Physics, Indian Institute of Science, Bangalore 560 012, India

Received 11 January 2002 / Accepted 4 June 2002

Abstract. Many spiral galaxies show a large-scale asymmetry with a $\cos \phi$ dependence in their rotation curves as well as in their morphology, such as M 101 and NGC 628. We show that both these features can be explained by the response of a galactic disk to an imposed lopsided halo potential. A perturbation potential of 5% is deduced for the morphologically lopsided galaxies in the Rix & Zaritsky (1995) sample. This is shown to result in a difference of 10% or \geq 20–30 km s⁻¹ in the rotation velocity on the two sides of the major axis. Interestingly, the observed isophotal asymmetry in a typical spiral galaxy is not much smaller and it results in a velocity asymmetry of 7% or \sim 14–21 km s⁻¹. Hence, we predict that most spiral galaxies show a fairly significant rotational asymmetry. The rotation velocity is shown to be maximum along the elongated isophote – in agreement with the observations along the SW in M 101, while it is minimum along the opposite direction. This result leads to the distinctive asymmetric shape of the rotation curve which rises more steeply in one half of the galaxy than the other, as observed by Swaters et al. (1999). This shape is shown to be a robust feature and would result for any centrally concentrated disk. The net disk lopsidedness and hence the asymmetry in the rotation curve is predicted to increase with radius and hence can be best studied using HI gas as the tracer.

Key words. galaxies: kinematics and dynamics – galaxies: ISM – galaxies: spiral – galaxies: structure – galaxies: halos

1. Introduction

The rotation curve of a spiral galaxy measures the variation of the rotation speed with radius in a galactic disk. This kinematic information is of crucial importance in understanding the structure and dynamics of spiral galaxies (e.g. Sofue & Rubin 2001). Typically, the rotation curve is assumed to be azimuthally symmetric for simplicity and this is used to obtain the corresponding axisymmetric mass distribution in a galaxy that is supported rotationally (e.g., Binney & Tremaine 1987).

The observed rotation curves in spiral galaxies, however, often show a deviation from a smooth circular rotation w.r.t. the galactic centre. The local deviations of a few km s⁻¹ are well-known (Shane & Bieger-Smith 1966) and are believed to be due to the streaming motions associated with spiral features. What is not so well-appreciated is that the rotation curves in many spiral galaxies show large-scale or global asymmetry such that the shape and the maximum velocity are different in the two halves of a galaxy, as for example in M 101 (Mihalas & Binney 1980). This indicates an underlying mass asymmetry in the galaxy. The global asymmetry of rotation curves is not so widely recognized because the observational data are generally averaged out to present an artificially "axisymmetric" rotation curve so that the precious information on the weak azimuthal asymmetry in the observed rotation curve is lost. Hence only the highly asymmetric cases such as M101 are recognized as having a global asymmetry. Further, even when large rotational asymmetry is noted in other individual galaxies it has been attributed to arise not due to underlying mass asymmetry but to other processes such as, due to absorption as in NGC 6181 (Burbidge et al. 1965), or due to an ejection from the centre as in NGC 4088 (Carozzi-Meyssonnier 1978).

Interestingly, all the nearby galaxies where the kinematics can be studied with good resolution, the rotation curve is observed to be azimuthally asymmetric, as for example in M 31 (Simien et al. 1978), M 33 (Colin & Athanassoula 1981), M 81 (Rots 1975), and NGC 4321 (Knapen et al. 1993). Yet the fact that most galaxies show some asymmetry in their rotation curves is not generally well-known. One of the aims of this paper is to highlight this point and to stress that observers should publish the rotation curve along both the sides of the major axis, and if possible give the full, azimuthal plot.

The observed large-scale asymmetry of rotation curves in the two halves of a galactic disk was first noted and underlined for a number of galaxies by Huchtmeier (1975), who showed that the difference in the rotational velocities could be ≥20 km s⁻¹. A study of CO rotation curves by Sofue (1996) also illustrates such asymmetry in the inner part of the optical disk. A recent study of a large sample confirms that the rotation curve asymmetry is the norm rather than the exception (Kannappan & Fabricant 2001). In addition, in many cases the shape of the rotation curve in the two halves of a galaxy is observed to be asymmetric, with the curve rising faster in one half of the galaxy than the other half (Sancisi 1996; Swaters et al. 1999).

Recent near-IR observations have also revealed morphological asymmetry in the underlying old stellar disks in a large

^{*} e-mail: cjjog@physics.iisc.ernet.in

fraction of galaxies studied, and the magnitude of the various azimuthal Fourier components denoted by m has been measured (Block et al. 1994; Rix & Zaritsky 1995; Zaritsky & Rix 1997; Rudnick & Rix 1998), also see Conselice (1997), and Kornreich et al. (1998) who measure the asymmetry in an average way. The HI distribution also shows mass asymmetry as seen in the global profiles (Richter & Sancisi 1994; Haynes et al. 1998). The isophotal asymmetry indicates asymmetry in the underlying disk mass distribution. It has been proposed (e.g., Weinberg 1995; Jog 1997) that the mass asymmetry occurs as a disk repsonse to an imposed halo distortion, the latter arising say due to a galaxy interaction.

The origin of the asymmetry in the rotation curves has not been addressed theoretically so far. In this paper, we show that the global asymmetry in the rotation curves as well as morphology can be explained naturally as arising due to the response of stars and gas in a galactic disk to an imposed lopsided (m = 1)halo potential. We note that even a small lopsided perturbation potential results in highly disturbed kinematics (Weinberg 1995; Jog 1997), hence it is easy to detect kinematic signatures of lopsidedness, especially the asymmetry in the rotation curve. From the calculation of perturbed orbits, we show that along the major axis of an orbit, the rotation velocity is a maximum along the maximum magnitude of the perturbation potential and is a minimum along the opposite direction (Jog 1997). Such an asymmetry of the rotation velocity along the major axis of an orbit was also pointed out by Earn & Lynden-Bell (1996), and Syer & Tremaine (1998), though these authors do not apply this result to the rotation curve in a galaxy. A similar asymmetry in the rotation curve resulting from an imposed m = 2 potential was studied by Gerhard & Vietri (1986).

In this paper, we obtain the typical velocity differences for galaxies for a lopsided potential the value of which is deduced from the observed morphological asymmetry, and compare these with observed velocity asymmetry. We also obtain the results for the inverse case, namely from the observed velocity difference known for the few galaxies, we can deduce the lopsided potential giving rise to the rotational asymmetry. Further, we tie in the velocity asymmetry to the isophotal elongation. The maximum velocity is shown to be along the elongated isophotes, this result agrees with the observations of M 101. This correlation also allows us to explain the asymmetric shapes of the rotation curves observed in lopsided galaxies.

Section 2 contains the derivation of the asymmetric rotation curve for a flat rotation curve, and also for a general, power-law rotation curve. Applications of results to galaxies are given in Sect. 3. A few general points are discussed in Sect. 4, and the results from this paper are summarised in Sect. 5.

2. Asymmetry in rotation curve

2.1. Orbits

We use galactic cylindrical co-ordinates R, ϕ , and z. We assume the galactic disk to be azimuthally symmetric on which a small lopsided halo potential is imposed. The unperturbed potential, $\psi_0(R)$ is taken to have a logarithmic form for simplicity, and

because it describes the region of flat rotation curve:

$$\psi_0(R) = V_c^2 \ln R \tag{1}$$

where V_c is the constant rotational velocity. The perturbation potential $\psi_{lop}(R)$ is taken to be non-rotating and of the following form:

$$\psi_{\text{lop}}(R,\phi) = V_c^2 \epsilon_{\text{lop}} \cos \phi \tag{2}$$

where ϵ_{lop} is a small, constant dimensionless parameter, denoting the perturbation in the potential. The case of a rotating perturbation potential is treated in the Appendix A.

Using the first-order epicyclic theory, the equations of motion for R, the orbital radius, and V_{ϕ} , the azimuthal component of velocity for the perturbed closed orbits around R_0 , ϕ_0 are obtained to be (Jog 2000, Appendix A) respectively:

$$R = R_0 \left(1 - 2 \, \epsilon_{\text{lop}} \, \cos \phi_0 \right) \tag{3}$$

$$V_{\phi} = V_{\rm c} (1 + \epsilon_{\rm lop} \cos \phi_0). \tag{4}$$

Thus, the orbit is shortened along $\phi=0^\circ$ where the perturbation potential is a maximum (see Eq. (2)), and it is elongated along the opposite direction along the major axis, along $\phi=180^\circ$. Note that ΔV_ϕ , the velocity difference at the two ends of the major axis ($\phi=0^\circ$ and $\phi=180^\circ$, respectively) is equal to:

$$\Delta V_{\phi} = 2V_{\rm c}\epsilon_{\rm lop}.\tag{5}$$

Thus the % velocity difference is exactly twice that of the perturbation in the potential.

2.2. Isophotes

The mass distribution in a spiral galactic disk is observed to fall exponentially with radius (Freeman 1970):

$$\mu_{\rm un}(R) = \mu_0 \, \exp\left(-\frac{R}{R_{\rm exp}}\right) \tag{6}$$

where μ_0 is the central extrapolated surface density and $R_{\rm exp}$ is the scale length of the exponential disk. For the perturbed case, the resulting effective surface density of the perturbed orbits in an exponential disk is defined by (see Rix & Zaritsky 1995; Jog 1997) to be:

$$\mu(R,\phi) = \mu_0 \exp\left[-\frac{R}{R_{\rm exp}} \left(1 - \frac{\epsilon_{\rm iso}}{2} \cos \phi\right)\right]. \tag{7}$$

An isophote is defined to be a curve of constant intensity or surface density for a constant mass-to-light ratio. For a particular isophote, the term in brackets in Eq. (7) is a constant, and defines the parametric form of the isophote. Thus, the minimum radius of an isophote occurs along $\phi=180^\circ$, while the maximum extent occurs along the $\phi=0^\circ$. Physically this is because the surface density falls off exponentially with radius and hence an isophote must be elongated in regions which show local density enhancement (that is, along $\phi=0^\circ$, see Eq. (7)). This correlation is true for any centrally concentrated disk.

Note that the elongation in an isophote is opposite to the behaviour of an individual orbit (Sect. 2.1). The rotation velocity is a maximum along the short side of an orbit, that is, along $\phi = 0^0$ (see Eqs. (3), (4)), that is along the elongated side of the isophote. The last point is somewhat counter-intuitive and arises due to the self-gravity in the disk, and we show that it agrees with observations (Sect. 3.4).

The isophotal shapes for an exponential disk are given following the procedure as in Jog (1997), and Jog (2000). For such a disk, A_1/A_0 , the fractional amplitude of the m=1 azimuthal Fourier component of the surface brightness is obtained to be:

$$A_1/A_0 = \left| -\frac{\Delta R}{R} \frac{R}{R_{\rm exp}} \right| \tag{8}$$

where $\Delta R/R$ is the distortion in the isophote. The amplitude A_1/A_0 is related to $\epsilon_{\rm iso}$, the ellipticity of the isophote at R, as follows:

$$A_1/A_0 = \frac{\epsilon_{\rm iso}}{2} \frac{R}{R_{\rm exp}}.$$
 (9)

Because of the orbital velocity changes along an orbit, the associated surface density also changes as a function of the angle ϕ . By solving together the equations of perturbed motion, the continuity equation, and the effective surface density (Eq. (7)), we obtain the following relation between the perturbation parameter ϵ_{lop} in the potential, and the resulting asymmetry in the isophotes as denoted by ϵ_{iso} or by A_1/A_0 (see Jog 2000, Appendix A) to be:

$$\epsilon_{\rm iso}/\epsilon_{\rm lop} = 4\left(1 - \frac{1}{2}\frac{R_{\rm exp}}{R}\right)$$
 (10)

and,

$$\epsilon_{\text{lop}} = \frac{A_1/A_0}{\left(\frac{2R}{R}\right) - 1} \tag{11}$$

where the $R \ge R_{\rm exp}$ since the calculation of loop orbits is valid for this range only (Rix & Zaritsky 1995). The above equations are valid for a self-consistent disk response for the lopsided (m=1) perturbation halo component, which takes account of the negative disk response due to the disk self-gravity to the imposed potential. Thus the $\epsilon_{\rm lop}$ obtained in Eq. (11) is the net lopsided perturbation parameter that affects the disk, which is smaller by a reduction factor (<1) compared to the "original" value for the halo (Jog 1999; Jog 2000).

2.3. Orbits and Isophotes in a power-law rotation curve

We obtain the results for closed orbits and isophotes in a lopsided perturbation potential for an exponential disk which obeys a general, power-law rotation curve given by

$$V = V_{\rm c} \left(R/R_0 \right)^{\alpha} \tag{12}$$

where V_c is the azimuthal velocity at R_0 , and α is a non-zero small number (<1) and is the logarithmic slope of the rotation curve. The corresponding unperturbed potential can be obtained to be (e.g., Kuijken & Tremaine 1994):

$$\psi_0(R) = (V_c^2/2\alpha) (R/R_0)^{2\alpha}.$$
(13)

In this case, the epicyclic frequency, κ is given by $\kappa^2/\Omega^2 = 2(1 + \alpha)$. In analogy with the case of the flat rotation curve (Eq. (2)), we assume the perturbation halo potential in this case to be

$$\psi_{\text{lop}}(R,\phi) = \left[V_{\text{c}}(R/R_0)^{\alpha}\right]^2 \epsilon_{\text{lop}} \cos \phi. \tag{14}$$

Using the first-order epicyclic theory as in Jog (2000), we obtain the equations of motion for closed perturbed orbits around R_0 , ϕ_0 in this case to be:

$$R = R_0 \left[1 - 2\epsilon_{\text{lop}} \left(\frac{1 + \alpha}{1 + 2\alpha} \right) \cos \phi_0 \right]$$
 (15)

$$V_{\phi} = V_{\rm c} \left[1 + \epsilon_{\rm lop} \left(\frac{1}{1 + 2\alpha} \right) \cos \phi_0 \right]. \tag{16}$$

Hence, ΔV_{ϕ} , the difference on the two sides of the major axis in this case is:

$$\Delta V_{\phi} = 2V_{c}\epsilon_{lop} \left(\frac{1}{1+2\alpha}\right). \tag{17}$$

On comparing this with Eq. (5), it can be seen that the % velocity difference on the two ends of the major axis is smaller in this case by a factor of $1/(1 + 2\alpha)$ than the value for the flat rotation curve.

The rotational velocity is a maximum at $\phi = 0^{\circ}$ (Eq. (16)) which is along the minimum of the orbital radius (Eq. (15)). Hence following the discussion as in Sect. 2.2 it can be seen that in this case also the maximum rotational velocity will be along the elongated part of an isophote.

Following an analysis similar to that in Sect. 2.2, it can be shown that the ratio of the ellipticity of an isophote, ϵ_{iso} , to ϵ_{lop} in this case is given by:

$$\frac{\epsilon_{\rm iso}}{\epsilon_{\rm lop}} = 4 \left[\left(\frac{1+\alpha}{1+2\alpha} \right) - \frac{R_{\rm exp}}{2R} \right]$$
 (18)

Using the relation between $\epsilon_{\rm iso}$ and the lopsided amplitude A_1/A_0 (Eq. (9)), we get in this case:

$$\epsilon_{\text{lop}} = \frac{A_1/A_0}{\left[(2R/R_{\text{exp}}) \left(\frac{1+\alpha}{1+2\alpha} \right) - 1 \right]}$$
 (19)

Check that in the limit of $\alpha = 0$, the last two equations reduce to the Eqs. (10) and (11) respectively which are valid for a flat rotation curve, as expected.

3. Results

3.1. Resulting asymmetry in rotation velocity, ΔV_{ϕ}

From the observed isophotal disk asymmetry values, A_1/A_0 , at a radius 2.5 $R_{\rm exp}$ (Rix & Zaritsky 1995), we deduce the perturbation parameter $\epsilon_{\rm lop}$ (Eq. (11)) for the lopsided potential, and thus obtain the resulting asymmetry in the rotation velocity (Eq. (5)). We show below that even a small perturbation potential gives rise to a large kinematic asymmetry, hence it is easy to detect. For the typical morphologically lopsided galaxies in the Rix & Zaritsky (1995) sample, with $A_1/A_0 \ge 0.2$, the perturbation parameter $\epsilon_{\rm lop}$ is obtained to be ≥ 0.05 and the net

velocity asymmetry $\Delta V_{\phi} \geq 0.10 V_{\rm c}$, or $\geq 10\%$ of the maximum rotation velocity. Thus for a typical range of maximum rotational velocity of 200–300 km s⁻¹ for a giant spiral galaxy (Binney & Tremaine 1987), the resulting magnitude of velocity asymmetry lies in the range of \geq 20–30 km s⁻¹. Nearly a quarter of the sample in Rix & Zaritsky (1995) is strongly lopsided $A_1/A_0 \geq 0.3$, for which the velocity asymmetry is higher \sim 30–45 km s⁻¹. This is closer to the value of the velocity asymmetry observed in NGC 628 and in M 101 (Kamphuis 1993).

The sample studied by Zaritsky & Rix (1997) is larger, and shows the same typical values for morphological lopsidedness. However, the value of asymmetry given is an average over a radial range of 1.5–2.5 exponential disk radii, and hence we cannot use Eq. (11) directly to obtain the value of the lopsided potential for this sample.

An important point is that the average or typical value of isophotal asymmetry for the Rix & Zaritsky (1995) sample is $A_1/A_0 = 0.14$, which we note is not much smaller than the value they use to define a lopsided galaxy $(A_1/A_0 \ge 0.2)$. For this average asymmetry, the resulting typical ϵ_{lop} is = 0.035 and the typical velocity difference is 7% of the maximum rotation velocity, or 14–21 km s⁻¹. Thus we predict that most spiral galaxies show a fairly significant rotational asymmetry, that can be easily checked by future observations.

3.1.1. Comparison of ΔV_{ϕ} with observations

As a direct verification of our model, we consider the specific case of one galaxy, NGC 991, for which the observed values for both the asymmetry in morphology and that in kinematics are known in the same radial range. We use the observed A_1/A_0 amplitude values to obtain $\epsilon_{\rm lop}$, and hence calculate the resulting rotation velocity asymmetry. We show that this agrees well with the observed rotational asymmetry. This galaxy has a disk scalelength of 19.5" (Rix & Zaritsky 1995). The average amplitude for lopsidedness between 1.5–2.5 disk scalelengths, or at an average radius of 2 disk scalengths =37", is 0.224 (Zaritsky & Rix 1997).

The detailed kinematics for NGC 991 has been observed by Kornreich et al. (2000), see their Fig. 2. By fitting the observed rotation curve V_c sin i between 10"–100" using Eq. (12) we get the slope α of the rising rotation curve to be =0.36. Here i is the inclination angle. Using this, we apply Eq. (19) at a radius of 37", and thus obtain ϵ_{lop} , the lopsided perturbation parameter to be 0.104. Using Eq. (17), we predict the fractional difference or asymmetry in the rotation curve on the two sides of the major axis to be 0.12. The observed rotational asymmetry at this average radius is $\sim 5/35 = 0.14$. Note that this ratio is independent of the inclination angle i. Thus the predicted value of rotational asymmetry agrees to within 17% of the observed value, this supports our model.

Unfortunately at this time such a detailed comparison is not possible for more galaxies because of lack of near-IR photometric data and detailed kinematic data for the same galaxies (also see Sect. 3.2).

The results for the typical values of the rotation velocity asymmetry obtained (see Sect. 3.1) agree well with the average

measurement of the rotation curve asymmetry of 4–10% for a sample of 9 Sa galaxies by Kornreich et al. (2001), which as per our model covers the range of weak to typical lopsided galaxies. These galaxies show little morphological asymmetry in the inner/optical disk but show a large kinematical asymmetry in HI in the outer region. In contrast, the values for the rotation curve asymmetry are much higher in the study of nine morphologically asymmetric galaxies by Kornreich et al. (2000), see their Table 4. In that work, 3 out of nine galaxies show strong asymmetry (>10%) in the rotation curve while the rest show weak asymmetry of (<10%). This confirms our picture that the kinematic and morphological lopsidedness in a galactic disk are causally related.

Note that the above asymmetry is the maximum that can be observed when the viewing angle is the most favourable, namely along the minor axis of the galaxy (90°–270°), so that the rotation velocity at the ends of the major axis (see Eq. (5)) is along the line of sight. The magnitude for any other orientation is smaller, and in the extreme opposite case when the line of sight is along the major axis, no asymmetry in rotation velocity is observed.

3.2. Lopsided Potential from observed ΔV_{ϕ} : Inverse application

The observed velocity difference at the two ends of the major axis yields a value for the perturbation parameter in the halo potential $\epsilon_{\rm lop}$ (see Eq. (5)) withought the necessity of detailed mapping. This is a lower limit on the actual value of $\epsilon_{\rm lop}$ because the observed ΔV_{ϕ} would be smaller than that given by Eq. (5) for any line of sight other than along the minor axis, which as we argued above is the most favourable for observing the velocity asymmetry.

This method is particularly important for the edge-on galaxies, like NGC 891, where the morphological asymmetry cannot be measured due to severe dust extinction, and the problem of unique de-convolution into non-axisymmetric features. This method is also applicable for inclined but largeangular size galaxies for which the measurement of optical asymmetry is time-consuming and has not been attempted so far, such as M 101 and NGC 628. This is despite the fact that such galaxies look highly disturbed in optical images. From the measured value of the velocity difference of $\sim 75 \text{ km s}^{-1}$ beyond 10' or $3R_{\rm exp}$ for M 101 (Kamphuis 1993), we obtain (using Eq. (5)) the lopsidedness in the halo potential, ϵ_{lop} to be =0.2. This is about 4 times larger than the value of 0.05 we derived (Sect. 3.1) for a typical morphologically lopsided galaxy in the Rix & Zaritsky (1995) sample. Similarly, for the observed velocity difference across the major axis of \sim 20–30 km s⁻¹ for NGC 628 (Kamphuis 1993), at a constant velocity of 200 km s⁻¹, we obtain $\epsilon_{lop} \sim 0.05-0.075$. These are upper limits on the actual asymmetry in the potential of both these galaxies since both these show strong evidence for gas infall at large radii which could cause kinematic asymmetry due to reasons other than the disk response to a lopsided halo potential.

An interesting application of this idea of obtaining the lopsidedness in the halo potential from the observed velocity asymmetry is for the case of the Milky Way. It is well-known that the rotation curves in the northern and southern hemispheres in the Galaxy show a global asymmetry and the diference in the two values is $\sim 8 \text{ km s}^{-1}$ (Kerr 1964). Following the discussion in Sect. 3.1, it is shown below that if the observed global asymmetry in the rotation curve of 8 km s⁻¹ is to be attributed to the disk response to a lopsided halo potential, then our Galaxy is weakly lopsided. For the observed range of velocities of 230 to 260 km s⁻¹ between a radius of 4 to 8 kpc (Kerr 1964), and applying Eq. (12), we get the power-law index for the rotation curve to be 0.32. Hence for the observed velocity difference of 8 km s⁻¹ and $V_c = 260 \text{ km s}^{-1}$, Eq. (17) gives $\epsilon_{lop} = 0.02$. This is less than half the value of ~5% derived for the typical lopsided galaxy in the Rix & Zaritsky (1995) sample (see Sect. 3.1). The origin of the north/south rotation curve asymmetry in the Galaxy was first conjectured by Sancisi (1981) to be due to a lopsided distribution, though in a qualitative way.

The above inverse problem was done more rigorously from the full two-dimensional kinematic information for two galaxies by Schoenmakers et al. (1997). However the various Fourier (*m*) components are coupled and it is not possible to get a unique value of lopsided parameter for the potential from such an analysis. Our method of measuring asymmetry in the rotation curve has the benefit of being a very simple measurement, and is especially applicable for edge-on galaxies where the decomposition of kinematic data would be hard.

It would be worth comparing the value of the ϵ_{lop} as obtained from the rotation curve and that from the near-IR isophotal analysis. If these agree, then that would support our model. Unfortunately, the galaxies in the Rix & Zaritsky (1995) sample are chosen to be of small-angular size to allow a single CCD frame measurement, and only a few of these have kinematic data in the literature. Conversely, the nearby, large-angular size galaxies for which rotational asymmetry is studied such as M 101 do not have measured isophotal asymmetry values in the near-IR.

3.3. Dependence of asymmetry on radius and tracer

The magnitude of the lopsided distribution in old stars, A_1/A_0 , is observed to be important beyond 1.5 exponential disk radii and it increases with radius (Rix & Zaritsky 1995). The signal-to-noise ratio limited their measuements to only 2.5 exponential disk radii. The lopsided disk distribution was first observed in HI, at radii several times farther out than the optical disk as in M 101, and IC 342 (Baldwin et al. 1980), although the amplitudes of lopsidedness in HI distribution were not measured. Theoretical work has shown (Jog 1999) that the disk self-gravity resists the imposed lopsided gravitational field, and hence the net, self-consistent lopsided distribution is only important in the outer region of a galactic disk, beyond two exponential disk radii (Jog 2000) indicating the increasing dynamical importance of the halo compared to the disk at large radii. This agrees reasonably well with the near-IR observations of

Rix & Zaritsky (1995), and Zaritsky & Rix (1997) – the latter give an average value of the lopsided amplitudes between 1.5–2.5 exponential disk radii. The large kinematical asymmetry in HI in the outer region of galaxies that may show little morphological asymmetry in the inner or optical disk as observed by Kornreich et al. (2001) (see Sect. 3.1.1) also agrees with this prediction.

Thus, we note that the HI component can act as an excellent diagnostic of the halo lopsidedness, since it typically extends 2–3 times beyond the optical disk (e.g. Giovanelli & Haynes 1988). Hence we predict that the asymmetric rotation curve in a typical spiral galaxy will be most easily detected in the outer galactic disk, studied using HI as a tracer.

3.4. Correlation of velocity with isophotal orientation

In our model, the disk responds to the halo distortion, and hence the asymmetry in the rotation velocity and the isophotal elongation have a unique correlation such that the maximum rotation velocity is along the elongated side of the isophote as shown in Sect. 2.2. This prediction agrees with the rotation curve in M 101 which shows a maximum velocity along the southwest (Kamphuis 1993) along which the surface density is also higher, and along which the isophotes in the inner galaxy are elongated. This is also true for the case of IC 342 which has a high surface density along the NW (Baldwin et al. 1980), and the rotation curve along the W is higher by $\sim 20 \text{ km s}^{-1}$ than along the E (Sofue 1996). In order for the above correlation to be detected, it is implicitly assumed that the tracer exists upto the larger extent on the elongated side of the isophote so that the above asymmetry is manifested. The above correlation between the maximum of the rotation velocity and the isophotal elongation is also valid for a general, power-law rotation curve (Sect. 2.3), and for a perturbation potential with a nonzero pattern speed (Appendix A).

The orbital and isophotal elongation occur along the opposite directions of the major axis, as shown in Sect. 2.2. Since the observed quantity is the isophote rather than an orbit, we have given the above correlation between the maximum velocity and the elongation in the isophote. In contrast, the models for disk lopsidedness by Earn & Lynden-Bell (1996) and by Noordermeer et al. (2001), do not make the distinction between the elongation in the orbit and isophotes. They also show that the maximum velocity is along the "small side" of the orbit but they do not make any predictions about the maximum velocity and the isophotal orientation, which is the only quantity that may be directly verified from obsevations.

We note that some galaxies show the reverse result where the maximum velocity is seen along the less elongated side of the isophote such as along the SE in NGC 4565, or along the side with lower surface density such as along NE in NGC 253 (Sofue 1996). Our picture cannot explain these anomalous cases. Perhaps gas infall or a central bar could be responsible in severely disturbing the kinematics in these cases.

In some galaxies, there is an additional complication namely the sense of elongation is in opposite directions in the inner and the outer regions of the galaxy. This is true for example in M 101 where the isophotes in optical or isodensity contours for HI are elongated along the SW in the inner region, while in the outer region the HI contours are elongated in the opposite direction, namely the NE. This can be explained naturally in our model of a galactic disk respoding to an imposed halo potential, which is probably generated via galaxy encounters. This is because the subsequent galaxy encounters are un-correlated, therefore the lopsidedness in different radial regions of a galaxy halo and hence the net disk response may show different orientation as argued by Jog (1997). In this case, the rotation curve on one side of a major axis would change from being a maximum at a lower radius to a minimum at a higher radius, and hence we argue that the resulting rotation curve in this case would have a "braided" appearance. It would be interesting to check this with the full data covering all azimuthal points measured in future, say for M 101.

The above discussion on the correlation between isophotes and rotation velocity is applicable to galaxies with nested, oval or egg-shaped isophotes such as M 101 which arise due to a constant phase with radius of the halo potential as shown by Jog (1997). In contrast, the galaxies with a strong radial dependence of phase give one-armed spirals such as M 51 or NGC 4254. In the latter case the velocity will be maximum along different azimuthal angles at different radii since the major axis orientation changes with radius. Here too the maximum of the surface density would coincide with the elongation in the arm and we expect the velocity to be a maximum along the longer and more prominent arm, as along the NE in M 51. Unfortunately, only the average rotation curves for galaxies are given in the literature. We urge the observers to publish full, 2-D rotation curves which will allow a comparison of the above prediction with observations.

3.5. Asymmetric shapes of rotation curves

Recent detailed kinematical study of HI distribution in galaxies shows distinctive shapes of rotation curves in the two halves, such that in one half of the galaxy the rotation curve rises slowly than in the other half, and reaches the flat part at a larger radius (Sancisi 1996; Swaters et al. 1999). In retrospect, this asymmetry in shape is also seen in the earlier work where the rotation curve on the two sides of a major axis was measured (e.g. Huchtmeier 1975; Sofue 1996). We also note that the slow rising part is observed to end in a higher value of the flat rotation curve, and we argue below that this can be explained physically in terms of the response of a centrally concentrated galactic disk.

As shown in Sect. 2.3, for an exponential disk with a rising rotation curve, the maximum rotation velocity occurs along the direction of elongataion of an isophote. Thus, the maximum velocity will be reached at a larger radial distance from the galactic centre. The rotation curve would therefore increase gradually and have a smaller slope on this side of the major axis, where the rotational velocity is higher. Thus we can give a physical explanation as to why the slow rising part of a rotation curve ends in a higher value of the flat rotation velocity

as observed by Swaters et al. (1999), and it occurs at a larger radius in the disk. Since the correlation between the maximum velocity and the sense of elongation of an isophote is valid for any centrally concentrated disk (see Sect. 2.2), hence the above argument about the shape of the rotation curve is valid for any realistic, centrally concentrated disk.

4. Discussion

4.1. Asymmetry in galaxies in groups

In our model, the asymmetry in a galactic disk results from the self-consistent disk response to a halo distortion. The latter is most likely to arise in a tidal enclounter between galaxies as shown by the work of Weinberg (1995). The galaxies in a group undergo more frequent encounters than the field case and with a similar relative velocity, hence we expect a large fraction of galaxies in groups to exhibit lopsided distribution. This prediction is confirmed from the observations on Hickson group galaxies (Rubin et al. 1991) where ≥50% of galaxies show lopsided rotation curves. This is much larger than the case of field spiral galaxies where only ~25% show asymmetric rotation curves (Rubin et al. 1999; Sofue & Rubin 2001). The observations of rotation curves of 30 galaxies in 20 Hickson compact groups by Nishiura et al. (2001) confirms the above result that asymmetric rotation curves are more frequently seen in these galaxies than in the field spiral galaxies.

A study of five major spirals in the nearby Sculptor group of galaxies (Schoenmakers 2000) shows that all five show kinematic lopsidedness while two are globally elongated or are morphologically asymmetric. This is higher than the $\sim\!\!30\%$ of galaxies showing morphological lopsided distribution in the field case (Rix & Zaritsky 1995). This confirms our argument that the percentage of galaxies showing lopsided distribution is higher in groups.

In comparing the field versus the group cases, it should be remembered that the adopted definition of what constitutes lopsidedness is somewhat arbitrary in each paper. However, since the discrepancy between the field and the group cases is large, it probably points to a genuine difference between the two cases.

4.2. Morphological vs. kinematical lopsidedness

There has been some discussion in the literature as to whether the observed morphological and kinematical lopsidedness in a disk are correlated or not. Richter & Sancisi (1994) argue that the two are correlated except for exceptional cases like NGC 4395. This dwarf galaxy shows no asymmetry in morphology in stars and HI but does show a kinematical lopsidedness (Swaters et al. 1999). The reverse is also true for a number of dwarf galaxies which may show no kinematic asymmetry but do show morphological asymmetry (Swaters 1999). We note that these are dwarf galaxies, and it is possible that for these galaxies the model of an off-centre disk in a halo with retrograde orbits (Noordermeer et al. 2001) may apply, where the two forms of lopsidedness may not be correlated. This model requires the disk to be within the flat density, central core of the halo and hence is valid for late-type dwarf galaxies only.

We note that in their model, the resulting disk lopsided distribution is only seen in the inner two disk-scale lengths, hence their model is not valid for the vast majority of large spiral galaxies which show lopsided distribution in HI at radii far outside the optical region (Baldwin et al. 1980) – that is, at several times the disk scale-length. Their model also cannot explain the increasing disk lopsidedness in stars beyond 2 disk scale-lengths as observed for giant spirals by Rix & Zaritsky (1995).

Kornreich et al. (2000) have observed nine face-on, giant spiral galaxies and have argued that the different indicators of morphological and kinematical asymmetry are not well-correlated, except that the morphological asymmetry is correlated with the asymmetry in the position angle differences. The lack of correlation could be due to the fact that their indicators of lopsidedness denote average quantities. Further, their definition of morphological asymmetry (as developed by Kornreich et al. 1998) is not correct since it would consider a one-armed spiral such as NGC 2326 to be symmetric, whereas Jog (1997) has shown these to be asymmetric with a phase that varies with the radius. Thus some of the galaxies they classify as having morphological symmetry are actually asymmetric. This could partly explain the discrepancy they observe.

The origin of lopsidedness in the few giant giant spirals which show little optical asymmetry but show kinematical asymmetry in HI, and have counter-rotating cores such as NGC 4138 (Kornreich et al. 2001), could be attributed to the counter-rotation as in the model for lopsidedness developed by Sellwood & Merritt (1994). Or this behaviour could be explained by the fact that HI being at a larger radius is a better tracer of lopsided distribution than the stars in the inner disk since the net disk lopsidedness increases with radius in our model (see Sect. 3.3).

Physically it is hard to see how in general the two measures of lopsidedness could be un-correlated in a giant spiral galaxy since the two would be coupled via the continuity eqaution (see Jog 1997). However, in some cases, where there is another source of kinematic disturbance as say due to gas infall at large radii (van der Hulst & Sancisi 1988), the gas kinematics may be disturbed without affecting the mass distribution significantly. This is why the lopsided potential derived from the observed velocity difference in M 101 (Sect. 3.2) gives an upper bound to the actual value.

Finally, we point out a couple of caveats that need to be kept in mind when measuring the asymmetry. First, in order to see if the rotation curve is symmetric or not, it must be compared upto the same radius and in the same tracer on both the sides of a major axis. When this is not done, it could lead to a spurious claim that the rotation is symmetric, as Noordermeer et al. (2001) claim to be true for NGC 891. Actually the rotation curve is measured upto different radii on the two sides of the major axis (Swaters et al. 1997), and hence is definitely asymmetric on a global scale. Upto the last common radius on the two sides, the rotation curve however is symmetric. Similarly, in NGC 6946, the HI extends much farther out (to 25% larger radius) along the NE along the major axis than the SW, hence the rotation curve can only be defined upto a smaller radius

along the SW (Carignan et al. 1990). Hence, globally the rotation curve is asymmetric in NGC 6946.

The other point is that, the net lopsidedness is predicted to be higher at larger radii (Jog 1999), hence it is expected to be more easily seen in HI since it extends out to a larger radius than do the stars. This is in fact confirmed from the study of Kornreich et al. (2001), see Sect. 3.3. Hence, when comparing the lopsidedness of different galaxies, it is not correct to compare the asymmetry in stars measured upto a smaller radius with the asymmetry in HI measured upto a much larger radius.

5. Conclusions

We obtain the self-consistent response of an exponential galactic disk to an imposed lopsided halo potential, and show that the disk exhibits both morphological lopsidedness and an asymmetric rotation curve. We study the case of a disk with a flat rotation curve, as well as a disk with a general, power-law rotation curve. The main results obtained are:

- 1. The % velocity asymmetry in the rotation curve is twice that of the perturbation in the potential. Hence, even a small perturbation potential of a few % results in a significant asymmetry in the rotation curve.
- 2. From the observed isophotal asymmetry, it is predicted that the *typical* spiral galaxies will show an asymmetry in the rotation velocity of 14–21 km s⁻¹ which should be easily detectable.

For NGC 991, the calculated velocity asymmetry from the observed isophotal lopsidedness is shown to agree fairly well with the observed asymmetry in the rotation curve, this confirms our model.

We show that if the well-known North/South asymmetry of the rotation curve of the Galaxy is attributed to the disk response to a halo perturbation, then the Galaxy is a weakly lopsided galaxy with a perturbation potential of 2%.

- 3. The rotation velocity is shown to be a maximum along the elongated isophote, in agreement with the observation for example along the SW in M 101. Using this correlation, we can explain the observed, asymmetric shape of the rotation curves is galaxies in a natural way.
- 4. A tracer at larger radii, such as HI gas, will show a larger rotational asymmetry, and hence will be a good diagnostic of the lopsided halo potential.

We hope the present paper will motivate future observational papers to give full azimuthal rotation data in galaxies, which will lead to a better understanding of galaxy asymmetry.

Acknowledgements. I would like to thank the referee for many constructive comments which have greatly improved the paper, and also led to the addition of the case of a general power-law rotation curve, and also the case of a rotating potential.

Appendix A: Perturbation halo potential with a non-zero pattern speed

Here we derive the equations for the closed orbits and the isophotes in an exponential disk perturbed by a small lopsided

potential ψ_{lop} which has a small, non-zero, constant pattern speed of rotation Ω_p . The unperturbed disk potential is denoted by $\psi_0(R)$. The perturbation potential can be written as:

$$\psi_{\text{lop}}(R,\phi) = \psi_{\text{pert}}(R) \cos \phi$$
 (A.1)

where $\psi_{\text{pert}}(R)$ is the magnitude of the lopsided perturbation potential.

A perturbed orbit around the initial circular orbit at R_0 may be written as: $R = R_0 + \delta R$ and $\phi = \phi_0 + \delta \phi$. From the equation of motion in the rotating frame for an unperturbed disk (Binney & Tremaine 1987, Chapter 3.3), we get

$$\left(\frac{\mathrm{d}\psi_0}{\mathrm{d}R}\right)_{R_0} = R_0 \left(\mathrm{d}\phi_0/\mathrm{d}t + \Omega_\mathrm{p}\right)^2. \tag{A.2}$$

For a disk in a rotational equilibrium, the angular velocity Ω_0 at R_0 is given by:

$$\Omega_0 = \left[\frac{1}{R_0} \left(\frac{\mathrm{d}\psi_0}{\mathrm{d}R} \right)_{R_0} \right]^{1/2}. \tag{A.3}$$

Hence the angular velocity of the guiding centre at R_0 in the rotating frame is given by $d\phi_0/dt = \Omega_0 - \Omega_p$. On integrating with time, and appropriately choosing t = 0, we get $\phi_0 = (\Omega_0 - \Omega_p)t$.

Following the treatment for the first-order epicyclic theory for a rotating frame with a small, non-zero pattern speed from Binney & Tremaine (1987), we get the following coupled equations of motion for δR and $\delta \phi$:

$$\begin{split} \frac{\mathrm{d}^2 \delta R}{\mathrm{d}t^2} &= -\delta R \left(3\Omega_0^2 + \frac{\mathrm{d}^2 \psi_0}{\mathrm{d}R^2}_{(\text{at }R_0)} \right) \\ - \left(\frac{\Omega_0}{\Omega_0 - \Omega_\mathrm{p}} \frac{2\psi_\mathrm{pert}(R_0)}{R_0} + \frac{\mathrm{d}\psi_\mathrm{pert}}{\mathrm{d}R}_{(\text{at }R_0)} \right) \cos(\Omega_0 - \Omega_\mathrm{p}) t \ \ (\mathrm{A.4}) \end{split}$$

and

$$R_0 \frac{\mathrm{d}^2 \delta \phi}{\mathrm{d}t^2} + 2\Omega_0 \frac{\mathrm{d}\delta R}{\mathrm{d}t} = \frac{\psi_{\text{pert}}(R_0)}{R_0} \sin(\Omega_0 - \Omega_{\text{p}})t. \tag{A.5}$$

The first term in the parantheses on the right hand side of Eq. (A.4) is the square of the standard first order epicyclic frequency, κ , at R_0 . From the theory of a driven oscillator (e.g., Symon 1960), these may be solved to give the following solutions for the closed orbits in the rest frame of the rotating perturbation potential:

$$R = R_0 - \frac{\left(\frac{\Omega_0}{\Omega_0 - \Omega_p} \frac{2\psi_{\text{pert}}(R_0)}{R_0} + \left(\frac{\text{d}\psi_{\text{pert}}}{\text{d}R}\right)_{(\text{at }R_0)}\right) \cos(\Omega_0 - \Omega_p)t}{\kappa^2 - (\Omega_0 - \Omega_p)^2} \cdot (A.6)$$

Hence, V_R , the perturbed radial velocity along this orbit is given by

$$V_{\rm R} = \frac{\left(\frac{2\Omega_0 \psi_{\rm pert}(R_0)}{R_0} + (\Omega_0 - \Omega_{\rm p}) \left(\frac{\mathrm{d}\psi_{\rm pert}}{\mathrm{d}R}\right)_{(\text{at }R_0)}\right) \sin(\Omega_0 - \Omega_{\rm p})t}{\kappa^2 - (\Omega_0 - \Omega_{\rm p})^2} \cdot (A.7)$$

The net azimuthal velocity, V_{ϕ} , is given by:

$$V_{\phi} = V_{c} + \frac{\Omega_{0} \left(\frac{d\psi_{pert}}{dR}\right)_{(at R_{0})}}{\kappa^{2} - (\Omega_{0} - \Omega_{p})^{2}} \cos(\Omega_{0} - \Omega_{p})t$$

$$+ \frac{\left(2\Omega_{0}^{2} - \left[\kappa^{2} - (\Omega_{0} - \Omega_{p})^{2}\right]\right) \psi_{pert}(R_{0})}{R_{0}(\Omega_{0} - \Omega_{p})\left[\kappa^{2} - (\Omega_{0} - \Omega_{p})^{2}\right]} \cos(\Omega_{0} - \Omega_{p})t.(A.8)$$

Note that in the limit of $\Omega_{\rm p}=0$, and when $\psi_0=V_{\rm c}^2\ln R$ and $\psi_{\rm pert}=V_{\rm c}^2~\epsilon_{\rm lop}$, the above two equations reduce to the equations for velocity for a non-rotating perturbation potential as treated in Jog (2000), see their Eq. (A.10). The maximum rotational velocity occurs along $(\Omega_0-\Omega_{\rm p})t=0^\circ$, along which the perturbed orbit has a minimum extent (see Eq. (A.6)). Hence, following the same argument as in Sect. 2.2, it can be seen that in this case also the rotation velocity is a maximum along the elongated side of an isophote.

The above equation shows that a non-zero pattern speed Ω_p does leave a signature in the resulting rotational velocity that can be measured. In particular it can give rise to resonances which are particularly important at higher radii where Ω_0 is low ($\sim \Omega_p$), and where lopsided perturbation is more likely to occur (Jog 1999). We note that the recent theoretical work on longevity of lopsided potential (Ideta 2002) argues that the pattern speed is likely to be low. In any case, we have treated the case of a non-zero pattern speed here for the sake of completeness.

We next obtain the isophotes for a specific case for the sake of simplicity, where the unpertubed and perturbed potential are taken to be respectively:

$$\psi_0(R) = V_c^2 \ln R \tag{A.9}$$

$$\psi_{\text{lop}}(R,\phi) = V_c^2 \, \epsilon_{\text{lop}} \, \cos(\Omega_0 - \Omega_{\text{p}})t. \tag{A.10}$$

These are written in analogy with the non-rotating case treated in Sect. 2. We next apply the analysis as in Sect. 2 to the equations of motion obtained in this Appendix, and use the above choice of potentials. This gives the following relation between ϵ_{iso} , the ellipticity of an isophote and ϵ_{lop} :

$$\frac{\epsilon_{\text{iso}}}{\epsilon_{\text{lop}}} = \frac{4\Omega_0^2}{\kappa^2 - (\Omega_0 - \Omega_p)^2} \times \left[1 - \frac{R_{\text{exp}}}{R} \left(1 - \frac{2\Omega_0^2 - [\kappa^2 - (\Omega_0 - \Omega_p)^2]}{2\Omega_0 (\Omega_0 - \Omega_p)} \right) \right] \cdot (A.11)$$

Using the definition of ϵ_{iso} in terms of the amplitude A_1/A_0 (Eq. (9)), this gives:

$$\epsilon_{\text{lop}} = \frac{A_1/A_0}{\left[\frac{2\Omega_0^2}{\kappa^2 - (\Omega_0 - \Omega_p)^2}\right] \left[\frac{R}{R_{\text{exp}}} - \left(1 - \frac{2\Omega_0^2 - [\kappa^2 - (\Omega_0 - \Omega_p)^2]}{2\Omega_0(\Omega_0 - \Omega_p)}\right)\right]}$$
(A.12)

In the limit of $\Omega_p = 0$, the above two equations reduce to Eqs. (10) and (11) for the non-rotating potential, as expected.

References

Baldwin, J. E., Lynden-Bell, D., & Sancisi, R. 1980, MNRAS, 193, 313

Binney, J., & Tremaine, S. 1987, Galactic Dynamics (Princeton: Princeton University Press)

Block, D. L., Bertin, G., Stockton, A., et al. 1994, A&A, 288, 365
Burbidge, G., Bubidge, E., & Prendergast, K. H. 1965, ApJ, 142, 641
Carignan, C., Charbonneau, P., Boulanger, F., & Viallefond, F. 1990, A&A, 234, 43

Carozzi-Meyssonnier, N. 1978, A&A, 63, 415 Colin, J., & Athanassoula, E. 1981, A&A, 97, 63 Conselice, C. J. 1997, PASP, 109, 1251

Earn, D. J. D., & Lynden-Bell, D. 1996, MNRAS, 278, 395

Freeman, K. C. 1970, ApJ, 160, 811

Gerhard, O. E., & Vietri, M. 1986, MNRAS, 223, 377

Giovanelli, R., & Haynes, M. P. 1988, in Galactic and Extragalactic radio Astronomy, ed. G. L. Verschuur, & K. I. Kellermann, 2d ed. (New York: Springer), 522

Haynes, M. P., Hogg, D. E., Maddalena, R. J., Roberts, M. S., & van Zee, L. 1998, AJ, 115, 62

Huchtmeier, W. K. 1975, A&A, 45, 259

Ideta, M. 2002, ApJ, 568, 190

Jog, C. J. 1997, ApJ, 488, 642

Jog, C. J. 1999, ApJ, 522, 661

Jog, C. J. 2000, ApJ, 542, 216

Kamphuis, J. 1993, Ph.D. Thesis, University of Groningen

Kannappan, S. J., & Fabricant, D. G. 2001, in Galaxy disks and Disk galaxies, ed. G. Jose, S. J. Furies, & M. C. Enrico (ASP: San Fransisco), ASP Conf. Ser., 230, 449

Kerr, F. J. 1964, The Galaxy and the Magellanic Clouds, IAU Symp. 20, ed. F. J. Kerr, & A. W. Rodgers (Canberra: Australian Acad. Sci.), 81

Knapen, J. K., Cepa, J., Beckman, J. E., del Rio, M. S., & Pedlar, A. 1993, ApJ, 416, 563

Kornreich, D. A., Haynes, M. P., & Lovelace, R. V. E. 1998, AJ, 116, 2154

Kornreich, D. A., Haynes, M. P., Lovelace, R. V. E., & van Zee, L. 2000, AJ, 120, 139

Kornreich, D. A., Haynes, M. P., Jore, K. P., & Lovelace, R. V. E. 2001, AJ, 121, 1358

Kuijken, K., & Tremaine, S. 1994, ApJ, 421, 178

Mihalas, D., & Binney, J. 1980, Galactic Astronomy (San Francisco: Freeman)

Nishiura, S., Shimada, M., Ohyama, Y., Murayama, T., & Taniguchi, Y. 2000, AJ, 120, 1691

Noordermeer, E., Sparke, L. S., & Levine, S. E. 2001, MNRAS, 328, 1064

Richter, O.-G., & Sancisi, R. 1994, A&A, 290, L9

Rix, H.-W., & Zaritsky, D. 1995, ApJ, 447, 82

Rots, A. H. 1975, A&A, 45, 43

Rubin, V. C., Hunter, D. A., & Ford, W. K. Jr. 1991, ApJS, 76, 153

Rubin, V. C., Waterman, A. H., & Kenney, J. D. 1999, AJ, 118, 236

Rudnick, G., & Rix, H.-W. 1998, AJ, 116, 1163

Sancisi, R. 1981, in The Structure and Evolution of Normal Galaxies, ed. S. M. Fall, & D. Lynden-Bell (Cambridge: Cambridge Univ. Press), 149

Sancisi, R. 1996, in New Light on Galaxy Evolution, ed. R. Bender, & R. L. Davies (Dordrecht: Kluwer), 143

Schoenmakers, R. H. M. 2000, in Small galaxy groups (ASP: San Fransisco), ASP Conf. Ser., 209, 54

Schoenmakers, R. H. M., Franx, M., & de Zeeuw, P. T. 1997, MNRAS, 292, 349

Sellwood, J. A., & Merritt, D. 1994, ApJ, 425, 530

Shane, W. W., & Bieger-Smith, G. P. 1966, BAN, 18, 263

Simien, F., Pellet, A., Monnet, G., et al. 1978, A&A, 67, 73

Sofue, Y. 1996, ApJ, 458, 120

Sofue, Y., & Rubin, V. C. 2001, ARA&A, 39, 137

Swaters, R. A. 1999, Ph.D. Thesis, University of Groningen

Swaters, R. A., Sancisi, R., & van der Hulst, J. M. 1997, ApJ, 491, 140

Swaters, R. A., Schoenmakers, R. H. M., Sancisi, R., & Van Albada, T. S. 1999, MNRAS, 304, 330

Syer, D., & Tremaine, S. D. 1996, MNRAS, 281, 925

Symon, K. R. 1960, Mechanics (Reading: Addison-Wesley)

Van der Hulst, J. M., & Sancisi, R. 1988, AJ, 95, 1354

Weinberg, M. D. 1995, ApJ, 455, L31

Zaritsky, D., & Rix, H.-W. 1997, ApJ, 477, 118